

## STRUCTURAL FEATURES OF MONTMORILLONITE-SURFACTANT SYSTEMS: INFLUENCE OF SURFACTANT PACKING DENSITY AND MONTMORILLONITE SURFACE NATURE

Oksana Seitnazarova, Alisher Kalbaev, Nozim Mamataliev,  
Aziza Abdikamalova, Nursulu Najimova

*Institute of General and Inorganic Chemistry  
Academy of Sciences of the Republic of Uzbekistan  
77a Mirzo Ulugbek St., Tashkent 100170, Uzbekistan  
qalbaev.alisher.98@gmail.com (A.K.); oks\_seyt\_1986@mail.ru (O.S.);  
mamataliyev@gmail.com (N.M.); aziza.abdik@gmail.com (A.A.); najimovanursuluw1973@gmail.com (N.N.)*

*Received 11 January 2024*

*Accepted 26 May 2024*

*DOI: 10.59957/jctm.v60.i1.2025.5*

---

### ABSTRACT

*This study presents sorption investigations of complexes formed by dihexadecyldimethylammonium bromide (DHDAB) and hexadecyltrimethylammonium bromide (HDTMAB) with montmorillonite, revealing the high affinity of these complexes for the interlayer space of clay. The intercalation process involves several stages, including initial rapid saturation, the formation of saturation plateaus, and subsequent super-equivalent sorption linked to the development of multi-layered structures or micelle-like formations on the surface of clay plates. This sorption mechanism is similar for various cationic surfactants.*

*DHDAB, with two alkyl chains, exhibits a more complex intercalation dynamic compared to HDTMAB, which has only one chain, and shows higher saturation efficiency at early stages. The cation exchange capacity (CEC) of montmorillonite influences the intercalation process, with clays possessing lower CEC having fewer available sites for intercalation.*

*Adsorption of different amounts of surfactants results in crystalline structures with varying interlayer distances. The saturation level of exchangeable cations ( $n$ ) influences the interplanar distance, and increasing  $n$  leads to a reduction in the specific surface area of montmorillonite samples. The adsorption efficiency of methylene blue on montmorillonites depends on their cation exchange capacity, structure, and degree of surfactant saturation. However, excessive saturation may lead to decreased efficiency due to the blocking of interlayer space. These findings are significant for the development and optimization of montmorillonite-based materials for environmental sorption and purification.*

***Keywords:** montmorillonite, cation exchange capacity, intercalation, surfactants, dihexadecyldimethylammonium bromide, hexadecyltrimethylammonium bromide, adsorption, methylene blue, saturation degree.*

---

### INTRODUCTION

The relevance of researching the intercalation processes of organic surfactants (OS) into aluminosilicates, such as montmorillonite, is driven by several key factors. These studies hold significant value in the context of developing new materials, improving sorption characteristics, modifying surface properties, and expanding their industrial applications. Moreover, they contribute to a deeper understanding of the corresponding interactions.

The process of intercalating OS into the interlayer space of aluminosilicates provides a perspective for the development of new composite materials with enhanced characteristics, including improved mechanical strength, chemical resistance, and thermal stability. Aluminosilicates typically exhibit increased capacity for sorbing organic pollutants when modified with intercalated OS, making them promise for applications in environmental safety. The intercalation process can also significantly alter the surface characteristics of aluminosilicates, serving as a foundation for creating

new catalysts, sensors, or materials with unique optical properties.

The investigation of surfactant intercalation processes into montmorillonite and other aluminosilicates holds paramount significance for a deeper understanding of molecular and ionic interactions at the interface, which, in turn, profoundly influences the development of new materials and technologies.

To ensure compatibility between organic and inorganic components that are initially incompatible from a thermodynamic standpoint, and to facilitate the penetration of macromolecules into the interlayer spaces of silicate layers on the filler surface and between these layers, the adsorption process of various surfactants (surfactant) is employed [1 - 3]. The adsorption of bulk organic cations and desorption of sodium result in an increase in the distance between clay layers, a phenomenon typically detectable through X-ray structural analysis (XSA).

Studies on the sorption of “surfactant-clay” complexes with respect to organic compounds encompass a broad spectrum of research [4 - 7]. These complexes, creating a hydrophobic environment due to the long alkyl chain of adsorbed surfactants, exhibit high affinity for hydrophobic compounds. This renders them promising for use in wastewater treatment processes [8, 9], the fabrication of landfill geomembranes [10], and as effective barriers preventing the contamination of groundwater and aquifers with organic pollutants.

The main mechanism that is considered dominant in the sorption of hydrophobic organic compounds on surfactant-clay complexes is that they are partitioned between the organic phase formed by adsorbed surfactant [8]. It was believed that the sorption coefficient (the ratio of the substance concentration on the sorbent to its concentration in the solution) is directly proportional to the amount of adsorbed surfactant [9, 10]. However, studies have shown that the sorption characteristics of these complexes are highly dependent on their structure [11 - 18]. The sorption behaviour is extremely sensitive to the configuration of the components, and therefore the normalized sorption coefficient ( $K_{oc}$ ), based on the content of organic carbon, can vary significantly [19]. For example, studies by Smith and colleagues have shown that surfactant-clay complexes obtained from surfactants with longer alkyl chains have higher K values for organic compounds [20]. However, the sorption

coefficient can also vary depending on the amount of intercalated surfactant [21].

The structural characteristics of the molecular template, and consequently, the density of their arrangement in the space between layers, determine the spacing between silicate plates, ultimately influencing the ability of the surface layer to interact with various organic substances. Thus, favourable conditions are created for the incorporation of macromolecules into the gaps between layers. Theoretical studies dedicated to the influence of the structure of surfactant layers on the thermodynamic compatibility between surfactant molecules attached to the surface of silicate plates and the polymer explicitly highlight the decisive role of this aspect in the creation of nanocomposite materials based on polymers with nonpolar chains and layered silicates [22].

The aim of this study is to investigate the influence of the exchangeable cation capacity of montmorillonite, surfactant packing density on the surface and in the interlayer space of montmorillonite on the alteration of the structural characteristics of the obtained organobentonites.

To achieve this goal, it is essential to establish the relationship between the structure of surfactant molecules, their ability to adsorb on clay, the amount of adsorbed surfactants, the formation of organophilic layers in the interlayer spaces of montmorillonite, and the distance between silicate plates. On the other hand, it is crucial to elucidate the extent to which macromolecule intercalation is possible in these gaps.

## **EXPERIMENTAL**

### **Materials used**

Enriched samples of bentonite from the Krantau deposit (Republic of Karakalpakstan) were employed for the study, with montmorillonite purity not less than 94 %. The clay's cation exchange capacity was 104 meq 100 g<sup>-1</sup>. As modifiers, dihexadecyldimethylammonium bromide (DHDAB) with a purity exceeding 97 %, and hexadecyltrimethylammonium bromide (HDTMAB) with a purity exceeding 98 % (Sigma-Aldrich) were utilized.

### **Organobentonite synthesis**

For the modification process, samples of montmorillonite mineral material (MM) with varying

values of cation exchange capacity (CEC) were employed. The CEC values of the products were determined using the method described by Boeva et al., which allows for a more precise determination of MM's cation exchange capacity [23]. Different CEC values of MM were achieved by exchanging  $\text{Na}^+$  ions with  $\text{Li}^+$ . The ion saturation procedures with  $\text{Li}^+$  followed the methodology presented in the study [24]. As a result, samples with CEC values of 86 and 70 mEq 100 g<sup>-1</sup> were obtained and denoted for convenience as MM86 and MM70, respectively.

Prior to the modification of montmorillonite samples using surfactants (surfactant concentration), suspensions (5 g of montmorillonite in 300 mL of water) underwent homogenization using an ultrasonic disperser UZD - Vt (Russia) for 3 min.

Individual surfactant solutions were prepared by dissolving the required amount of surfactant in 100 mL of water at a temperature of  $70 \pm 1^\circ\text{C}$ , with constant stirring for one hour. The amount of surfactant in the solution varied in the range from 0.416 to 5.2 mmol per g of MM, from 0.344 to 4.3 mmol per g of MM86, and from 0.28 to 3.5 mmol per g of MM70. These values corresponded to a variation in the amount of surfactant 2.5 times less and 5 times more than the cation exchange capacity of each bentonite. Subsequently, surfactant solutions were added to clay suspensions while stirring. The resulting suspensions were stirred at  $70^\circ\text{C}$  for 4 h. Afterward, the solid phase was separated from the liquid via centrifugation (DM0412 Dlab). The solid phase was washed three times with distilled water and dried at  $80^\circ\text{C}$ . The dried samples were pulverized, and then sieved through a 154  $\mu\text{m}$  mesh.

#### **Determination of surfactant concentration in solution**

The determination of surfactant content in aqueous solutions can be achieved through the analysis of their optical density,  $D$  in UV and visible light. Individual surfactant molecules can absorb light, while micelles scatter it. The intensity of scattering and the spectrum depend on the size and quantity of micelles. For specific surfactant solutions (quaternary ammonium salts), a change in UV light absorption is observed upon reaching the critical micelle concentration. The key is to determine the concentration at which the optical density remains stable.

To determine the concentration of surfactant

remaining after intercalation, the systems' data were diluted from 10 to 100 times depending on the surfactant concentration. In this study, we opted for a modifier detection method based on the interaction of surfactants with dye molecule to ascertain the concentration.

One of the most effective methods for measuring surfactant concentration is based on the interaction of alkylammonium surfactants with dye molecules, particularly methyl orange (MO). Concentrations of DHDAB and HDTMAB were determined based on the correlation between the intensity of the absorption peak of the surfactant-MO complex and the surfactant concentration in the system. The diagnostic procedure stands out for its accessibility of chemical reagents, utilization of relatively basic instrumentation, the ability to accurately assess the quantity of surfactants in micelles, and high sensitivity in the quantitative evaluation of surfactants in solution.

Due to the diverse parameters affecting the spectral characteristics of the surfactant-MO complex, the calibration and concentration determination methodology was standardized. A MO indicator solution with a concentration of  $2.5 \times 10^{-5} \text{ mol L}^{-1}$  was employed. Similarly, samples of DHDAB and HDTMAB were prepared with specified surfactant concentration levels (ranging from  $10^{-3}$  to  $1.5 \text{ mmol L}^{-1}$ ). The solutions were prepared at a temperature of approximately  $70^\circ\text{C}$  with active stirring. To 5 mL of each surfactant -  $\text{H}_2\text{O}$  system, 5 mL of the MO solution was added. The analysed solution was placed in a quartz cuvette with a 1 cm layer width, followed by spectrophotometric analysis using distilled water as a reference.

#### **X-ray structural analysis**

To investigate structural changes during the modification of montmorillonite, MM using various surfactants, considering their concentration and the surface charge of MM, X-ray structural analyses were conducted using a PANalytical XPert<sup>3</sup> MRD, XL X-ray diffractometer. Samples for X-ray structural analysis was prepared by applying a suspension of modified clay onto a glass slide using a dispenser, followed by vacuum drying for 3 h at room temperature.

#### **Low-temperature nitrogen adsorption**

In this study, the low-temperature nitrogen adsorption method at 77 K was employed on a static adsorption

setup, Quantachrome Nova 1000 e, to determine the characteristics of the porous structure of bentonite samples. Prior to measurements, samples underwent vacuum pretreatment at 100°C for 12 h. The partial pressure of nitrogen varied in the range of 0.005 to 0.995  $P/P_0$  for nitrogen adsorption and desorption isotherms. The Brunauer-Emmett-Teller (BET), Langmuir, Dubinin-Radushkevich, DR, t-plot, As-plot methods were used for processing adsorption curves, determining micropore volume and average pore diameter, while the Barrett-Joyner-Halenda, BJH method was applied to assess mesopore volume. Size distribution of pore volume and area was determined using the Density Functional Theory, DFT and Barrett-Joyner-Halenda, BJH methods. The average pore diameter was calculated using the BET formula:  $D = 4 V/S$ , where  $V$  is the volume of adsorbed nitrogen.

#### Methylene blue adsorption from aqueous solutions

The adsorption capacity for methylene blue was measured by determining the optical density at the characteristic wavelength of 660 nm.

MB, a primary dye, has the chemical formula  $C_{16}H_{18}NSCl$  and a molecular mass of  $320 \text{ g mol}^{-1}$ . It presents itself as dark green crystals with a bronze sheen.

The process of determining the adsorption capacity comprised the following stages: initially, Methylene Blue solutions in water were prepared with concentrations ranging from 1 to  $150 \text{ mg L}^{-1}$ , and their optical density

was measured. Based on the obtained data, a calibration graph was constructed.

Subsequently, 0.025 g of the powder from the examined samples was added to 50 mL solutions of various concentrations. After gently shaking the solutions, they were left at rest to reach adsorption equilibrium, the time for which was determined based on the adsorption kinetics curve. Kinetic adsorption studies were conducted on one solution for each montmorillonite sample. After reaching equilibrium, the optical densities of the solutions were measured, and their concentrations were determined based on the calibration graph data. The resulting isotherms were characterized using the Langmuir equations at low values of equilibrium adsorption [25].

## RESULTS AND DISCUSSION

#### Surfactant sorption by bentonite

Electronic absorption spectra for the MO solution and the DHDAB-MO and HDTMAB-MO complexes are presented in Fig. 1 - 3. Calibration graphs were obtained based on the measured absorption peaks of the surfactant-MO complexes at a constant indicator concentration (Fig. 1). These data enable the determination of the modifier's quantity in the analysed system.

In a study, it was demonstrated that dimethyldioctadecylammonium iodide in an organic solvent exhibits absorption bands at 205 and 245 nm, associated

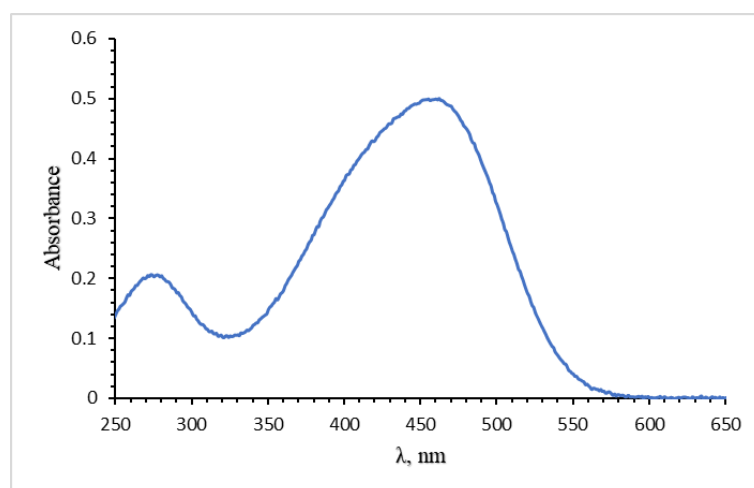


Fig. 1. Electronic absorption spectra of the MO solution ( $C = 1.25 \cdot 10^{-2} \text{ mmol L}^{-1}$ ).

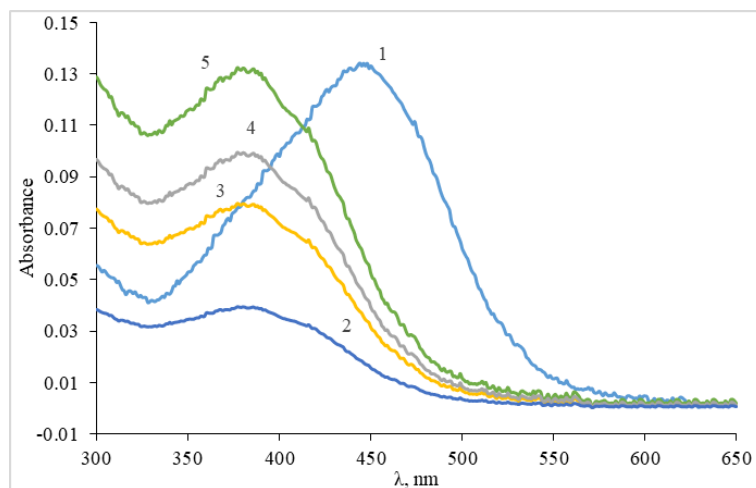


Fig. 2. Changes in peaks in the spectra of the DHDAB -MO system at surfactant concentrations in the system, mmol L<sup>-1</sup>: 1) 10<sup>-2</sup>; 2) 5\*10<sup>-2</sup>; 3) 0.1; 4) 0.5; 5) 1.

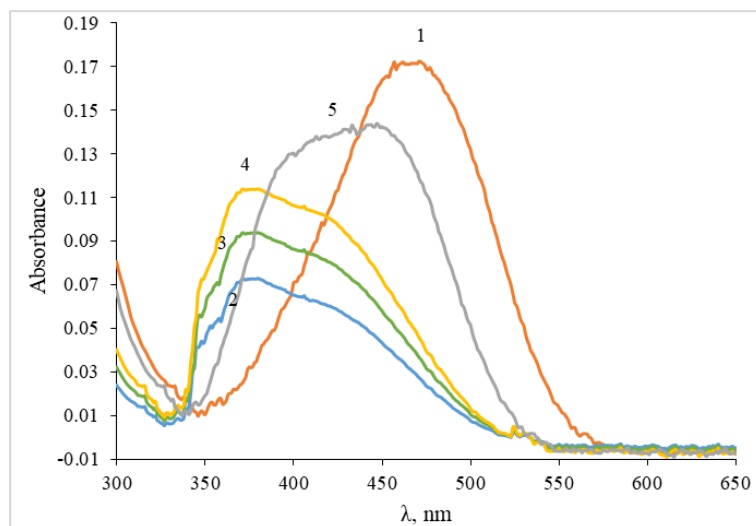


Fig. 3. Changes in peaks in the spectra of the DHDAB -MO system at surfactant concentrations in the system, mmol L<sup>-1</sup>: 1) 10<sup>-2</sup>; 2) 5\*10<sup>-2</sup>; 3) 0.1; 4) 0.5; 5) 1.

with electronic transitions of halide ions. However, in aqueous solutions, these bands are invisible due to water's light absorption.

Interaction between MO and surfactants causes a shift in the absorptive band of the dye, attributed to both electrostatic and hydrophobic interactions between molecules. According to [26], the entropic factor plays a pivotal role in the formation of such complexes.

The investigation of the interaction between

molecules of the compound  $(C_nH_{2n+1})_2(CH_3)_2N^+Br^-$  ( $n = 14 - 16$ ) with methyl orange, MO in an aqueous system revealed that the absorption spectrum of the formed complex manifests in the range of 370 - 390 nm, confirming the results of our study. A reduction in the concentration of bound MO dye to the surfactant by more than 50 times leads to a 20 nm shift in the absorption band towards shorter wavelengths [27]. This shift may be attributed to the reorientation of dye molecules on

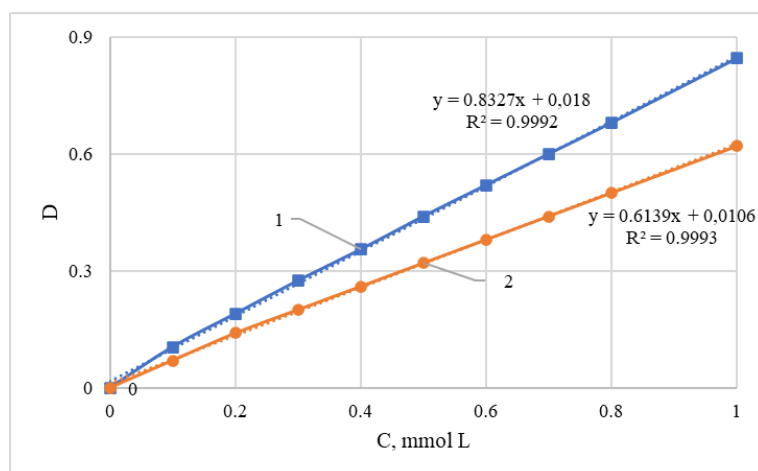


Fig. 4. Calibration graph of the dependence of optical density on the concentration of surfactants in the system: 1) DHDAB - MO; 2) HDTMAB - MO.

the micelle surface, leading to new forms of aggregation between the aromatic structures of neighbouring azobenzene molecules. Similar interaction mechanisms have been noted in systems involving complexes of polyethyleneimine and acylated derivatives of MO.

Fig. 5 presents curves illustrating the dependence of the quantity of intercalated DHDAB and HDTMAB on MM, MM86, and MM70 concerning the initial concentrations of surfactants. These curves exhibit notable distinctions among them. While MM and MM82 samples display curves characterized by three distinct regions, MM70 demonstrates curves reaching a maximum and then stabilizing with further increases in surfactant concentration for both compounds.

As seen in Fig. 5a, there is a rapid initial saturation of montmorillonite for both surfactants, indicating a high affinity of DHDAB cations for the interlayer space of the clay. In this concentration range (from 0 to 0.2 mmol L<sup>-1</sup>), the primary sorption mechanism is likely ion exchange. At residual concentrations in the solution from 0.2 to 0.65 mmol L<sup>-1</sup>, surfactant sorption onto montmorillonite slows down and practically stabilizes, indicating saturation of the interlayer space with surfactant cations.

With an increase in surfactant concentration in the solution from 0.65 mmol L<sup>-1</sup> and above, additional saturation of montmorillonite occurs, especially noticeable for DHDAB. Further excess sorption of DHDAB may be associated with the formation of a

multilayered structure on the external surface of clay plates rather than in the interlayer space.

For DHDAB, saturation of the interlayer space is achieved at a concentration of approximately 2.45 mmol g<sup>-1</sup> (with a residual surfactant concentration in the solution of 0.63 mmol L<sup>-1</sup>). This value is 2.36 times higher than the CEC of the clay (1.04 mmol g<sup>-1</sup>). In contrast, for HDTMAB, this indicator is reached at an adsorption quantity of about 1.55 mmol g<sup>-1</sup> (with a residual concentration in the solution of 0.83 mmol L<sup>-1</sup>), which exceeds the CEC of the clay by 1.49 times.

After the saturation of the interlayer space, additional surfactant sorption is observed, which may be associated with the formation of micelle-like structures on the surface of silicate plates or the formation of multilayers in the interplanar space. This mechanism has also been noted for other cationic surfactants [14], confirming the generalized nature of this process for different types of surfactants. The total amount of DHDAB and HDTMAB adsorbed in this clay sample is 4.0 and 3.4 mmol g<sup>-1</sup>, respectively, exceeding the clay CEC by 3.85 and 3.27 times.

During the desorption stage, after multiple washings with distilled water to zero surfactant concentration in the solution, the amount of remaining DHDAB in the interlayer space of the clay significantly exceeds the CEC. This confirms the hypothesis that some surfactant molecules replaced Na<sup>+</sup> cations at exchange positions, while another part is associated with them through forces

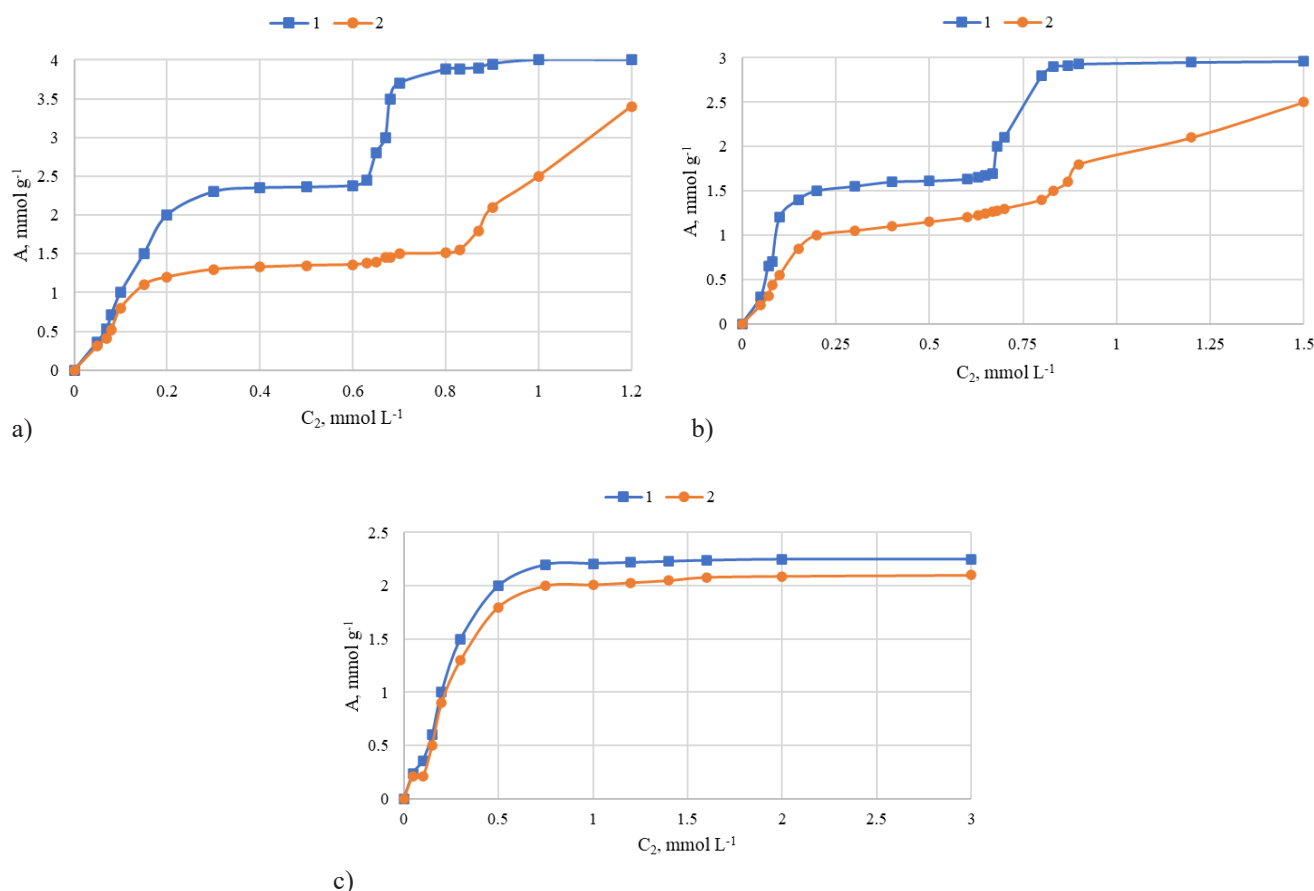


Fig. 5. Sorption isotherms of DDAB (1) and DTAB (2) on samples: MM (a), MM86 (b), MM70 (c).

of lyophilic (van der Waals) interaction.

Thus, the sorption of DHDAB and HDTMAB on the MM sample follows the classical three-stage process characteristic of cationic surfactants. The stages include initial rapid saturation, a plateau stage, and subsequent formation of micelle-like structures or multilayers. The data confirm that the length and number of alkyl chains in the surfactant molecule play a crucial role in the intercalation process. DHDAB, with its two chains, exhibits a more complex intercalation profile compared to HDTMAB. However, HDTMAB, with a single chain, is capable of intercalating into clay more efficiently in the early stages.

As in the previous case, rapid initial saturation of MM86 is observed for both surfactants. For montmorillonite with a CEC of 86 mmol 100 g<sup>-1</sup>, the initial absorption of DHDAB is significantly higher than that of HDTMAB. This may indicate a higher affinity of

DHDAB for this specific montmorillonite.

In both cases, a clear saturation plateau is observed, but for DHDAB, the plateau is reached at a solution concentration of approximately 0.4 mol L<sup>-1</sup>, while for HDTMAB, it starts at around 0.3 mol L<sup>-1</sup>. These differences may be attributed to the distinct structure and chemical properties of the surfactants. However, after the saturation of the interlayer space, additional surfactant sorption continues for both surfactants. Again, this may be associated with the formation of micelles on the surface of montmorillonite or multilayers in the interlayer space.

For montmorillonite with a CEC of 86 mmol 100 g<sup>-1</sup>, the saturation plateau for DHDAB occurs at a slightly higher surfactant concentration in the solution (0.70 versus 0.62 mol L<sup>-1</sup> for MM) compared to montmorillonite with a CEC of 104 mmol 100 g<sup>-1</sup>. This may suggest that montmorillonite with a lower

CEC has fewer available sites for DHDAB intercalation. However, the difference is less noticeable for HDTMAB ( $C_2 = 0.83$ ), indicating that the sorption mechanism of this surfactant is less sensitive to the CEC of montmorillonite.

With an increase in surfactant concentration in the solution from  $0.70 \text{ mmol L}^{-1}$  and above, there is additional saturation of montmorillonite. For DHDAB, saturation of the interlayer space is achieved at a concentration of approximately  $2.91 \text{ mmol g}^{-1}$  (at a residual surfactant concentration in the solution of  $0.87 \text{ mmol L}^{-1}$ ), while for HDTMAB, this value is reached at an adsorption quantity of about  $2.5 \text{ mmol g}^{-1}$  (at a residual concentration in the solution of  $1.5 \text{ mmol L}^{-1}$ ). The total amount of DHDAB and HDTMAB adsorbed on the clay sample is  $2.96$  and  $2.5 \text{ mmol g}^{-1}$ , respectively, exceeding the CEC of the clay by  $3.44$  and  $2.91$  times, respectively.

In the case of the MM70 sample, for both surfactants, initial absorption occurs rapidly, and by a concentration of  $0.2 \text{ mol L}^{-1}$ , surfactant sorption on montmorillonite significantly increases. As noted earlier, surfactant adsorption on this sample occurs in two stages. At a residual surfactant concentration of  $1 \text{ mmol L}^{-1}$ , the amount of adsorbed DHDAB reaches  $2.21 \text{ mmol g}^{-1}$ , which is approximately  $3.16$  times greater than the CEC of montmorillonite. For HDTMAB, at the same residual concentration in the solution, the adsorbed quantity reaches  $2.01 \text{ mmol g}^{-1}$ , approximately  $2.87$  times greater than the CEC of montmorillonite.

With an increase in surfactant concentration in the solution to  $3 \text{ mmol L}^{-1}$ , the adsorption of DHDAB remains practically unchanged, reaching  $2.25 \text{ mmol g}^{-1}$ , which is  $3.21$  times greater than the CEC of montmorillonite. Meanwhile, for HDTMAB, this value slightly increases to  $2.1 \text{ mmol g}^{-1}$ , constituting  $3.00$  times greater than the CEC of montmorillonite.

The sorption mechanisms of DHDAB and HDTMAB on montmorillonite with a CEC of  $70 \text{ mmol } 100 \text{ g}^{-1}$  are generally like those on montmorillonites with higher CEC. However, montmorillonite with a CEC of  $70 \text{ mmol } 100 \text{ g}^{-1}$  exhibits rapid saturation, which may be associated with a lower number of available interlayer sites for intercalation. There is also a slight difference in the affinity of surfactants to this montmorillonite, where DHDAB demonstrates slightly higher sorption compared to HDTMAB.

The difference in the sorption density of surfactants on these matrices can be inferred from the adsorption process and the charge properties of the matrices. For bentonites with reduced charge, it is considered that the distance between charged regions is greater. In low surfactant concentration regions (for MM70), surfactants predominantly attach through ion exchange, mainly associating with the charged regions of bentonite. As a result, such bentonites show reduced surfactant density. On the other hand, in high surfactant concentration regions, many surfactants attach in their molecular form due to hydrophobic interactions with surfactant chains. This reduces the space between attached surfactants. Additionally, electrostatic repulsion from charged parts causes some surfactants to spread to nearby uncharged areas. As the amount of surfactants increases, their packing density on bentonites with different layer charges becomes more homogeneous in this region. As a result of experimental studies, it was found that the enhancement factor of DHDAB over CEC for MM, MM86, and MM70 samples are  $3.85$ ,  $3.44$ , and  $3.21$ , respectively. Whereas for HDTMAB, these factors are  $3.26$ ,  $2.91$ , and  $3$  times, respectively. Whereas for HDTMAB, these coefficients are  $3.26$ ,  $2.91$ , and  $3$  times, respectively. Noticeably, the adsorption of HDTMAB is higher for the MM70 sample compared to MM86.

### Structure of intercalated montmorillonites

Fig. 6 presents X-ray diffractograms of selected MM samples. Data analysis revealed that the difference in cation exchange capacity leads to a change in the interlayer spacing. Thus, the main reflection of montmorillonite  $d_{001}$  for MM and MM86 is determined at levels of  $1.261$  and  $1.253 \text{ nm}$ , respectively. However, for MM70, the reflex demonstrates a shift towards a larger  $2\theta$  angle, with calculated values around  $1.199 \text{ nm}$ . It is assumed that the reduction in the concentration of hydrophilic exchange cations leads to a decrease in the volume of chemically bound water in the interlayer space, accompanied by a reduction in this space. Presumably, in this process, MM loses some of the adsorbed water, interlayer spaces are disrupted, and the pore space changes, significantly altering the surface acidity [28].

Using X-ray structural analysis methodology, the dependence of interlayer distance in MM on the amount of adsorbed surfactant was studied. Fig. 7 shows X-ray

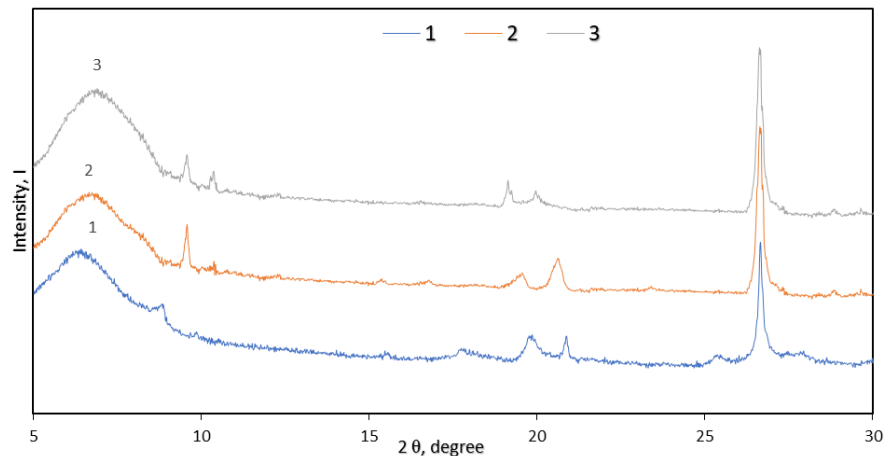


Fig. 6. X-ray diffraction patterns of the samples: 1) MM; 2) MM86; 3) MM70.

spectra of MM modified with various concentrations of DHDAB. The amount of adsorbed surfactant is presented as a fraction of the clay CEC, expressing the degree of clay saturation with the modifier.

In all cases, higher distances between basal surfaces of montmorillonite samples in the surfactant system were observed, indicating the intercalation of surfactants into the interlayer space of the original MM. Similar results were obtained when Na-montmorillonite interacted with various organic modifiers [29].

After adsorption of DHDAB on MM with a quantity of  $n = 1/4$ , new reflections with interlayer distances around 1.61 - 1.73 and 2.03 - 2.11 nm were noticed, while maintaining the peak for the original MM (1.23 nm). This suggests the presence of clay crystallites with different interlayer distances in the clay (mixed structure).

With an increase in the amount of DHDAB from  $n = 1/4$  to  $n = 1/2$ , the distribution of intensity between the two reflections changed. At the clay saturation level with the modifier  $n = 1/2$  or higher, the new reflection splits, forming an additional peak with about 2.23 nm, which becomes distinct at  $n = 1 \leq 1.25$ . With such filling (from  $n = 1/4$  to  $n = 1/2$ ), a pseudomonolayer structure of DHDAB between the layers of MM can be assumed. Increasing  $n$  to 3.8 shifts this peak to even smaller reflection angles, corresponding to an interlayer distance of 2.87 - 2.90 nm. In this case, a pseudobilayer structure of the intercalated surfactant can be suggested. However, the indicated values of

interlayer distance significantly differ from the results obtained earlier during the modification of MM with dihexadecyldimethylammonium bromide. This is likely primarily due to the characteristics of MM, and only then to the properties of the surfactants, considering that the compared surfactants are slightly different in nature and size.

Based on the analysis of X-ray diffraction patterns of modified montmorillonite (MM) in the presence of HDTMAB-B, it was found that during the sorption of HDTMAB-B in an amount of  $n = 0.25$ , a unique reflex with an interlayer distance fluctuating in the range of 1.51 - 1.58 nm is formed. This phenomenon contrasts with the data obtained using DHDAB. It is assumed that this difference may arise due to variations in the size of HDTMAB -B molecules.

The interaction of MM with HDTMAB in an amount of  $n = 0.5 - 0.6$  led to an expansion of the basal space in the sample to 1.84 - 1.85 nm, corresponding to previously obtained data by other authors [29].

With an increase in the concentration of HDTMAB - B to  $n = 3.27$ , an increase in the interlayer distance to values between 2.21 and 2.34 nm is observed. It is noteworthy that in a published work, where the interaction of MM with hexadecyltrimethylammonium bromide is considered, there is mention of a reflex with an interplanar distance of 3.6 nm. However, despite the similar characteristics of the original montmorillonite and the object of our study, in our data, the maximally

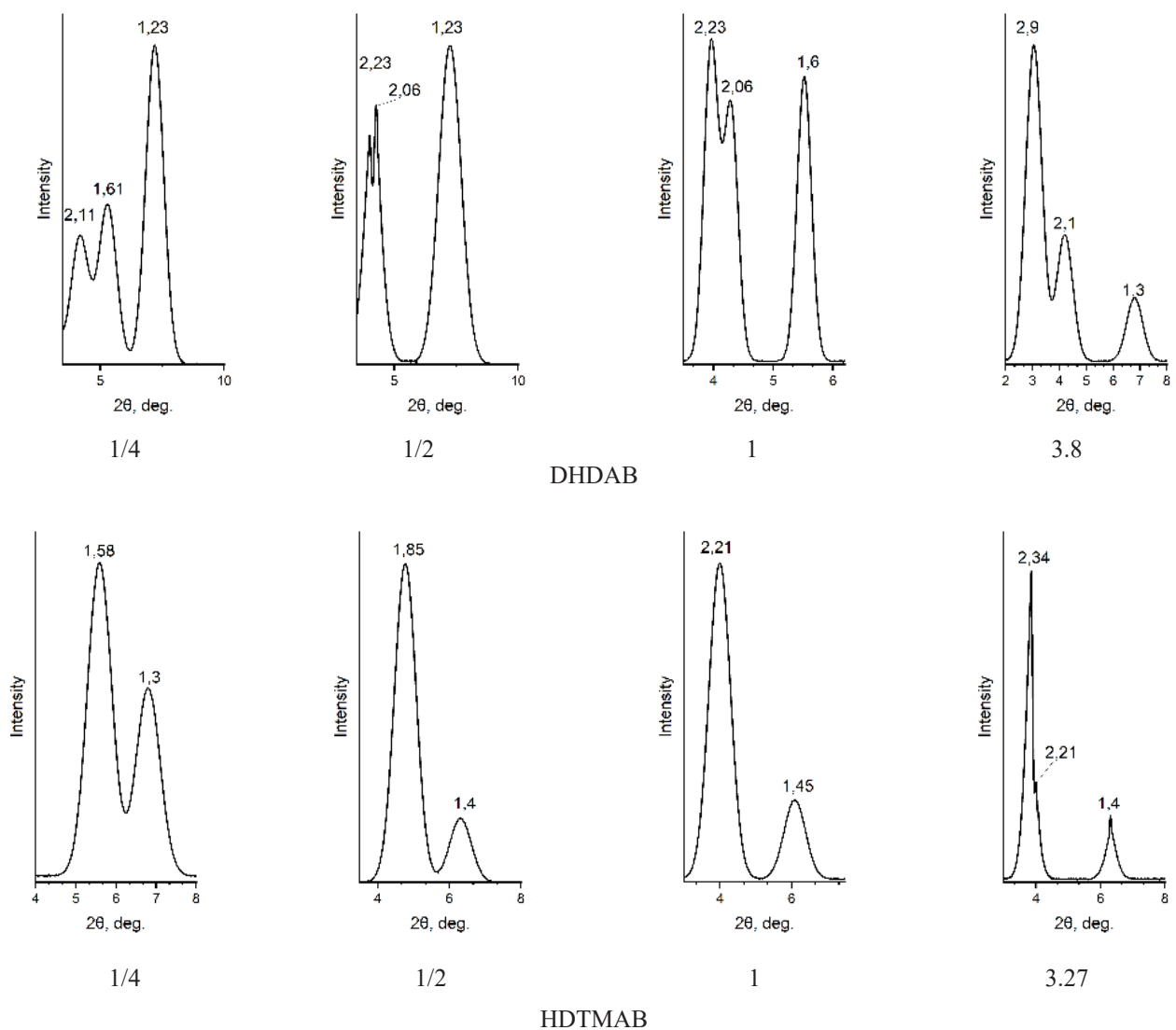


Fig. 7. X-ray diffraction patterns of the organomodified sample MM.

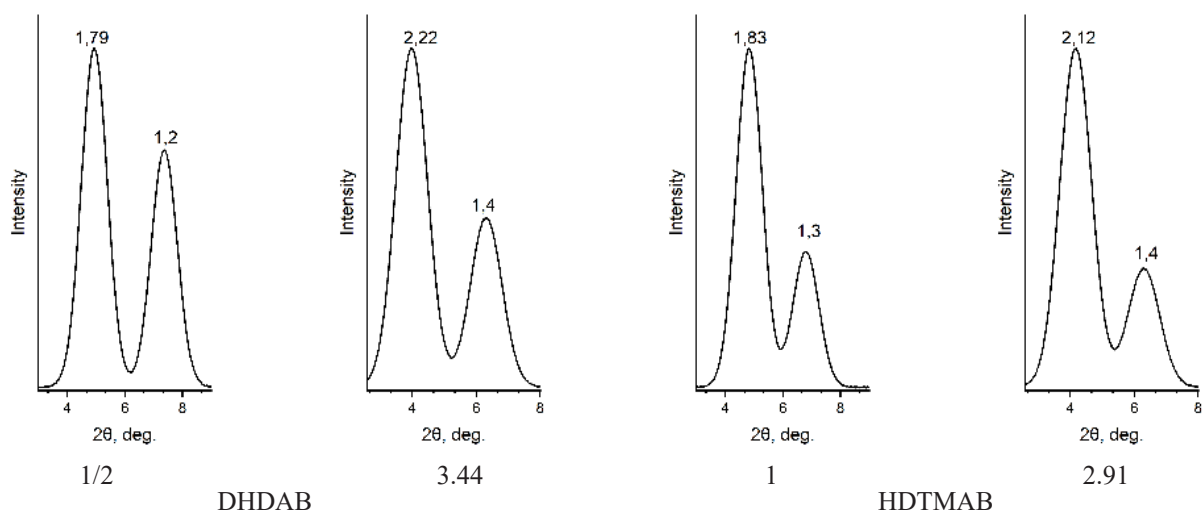


Fig. 8. X-ray diffraction patterns of the organomodified sample MM86.

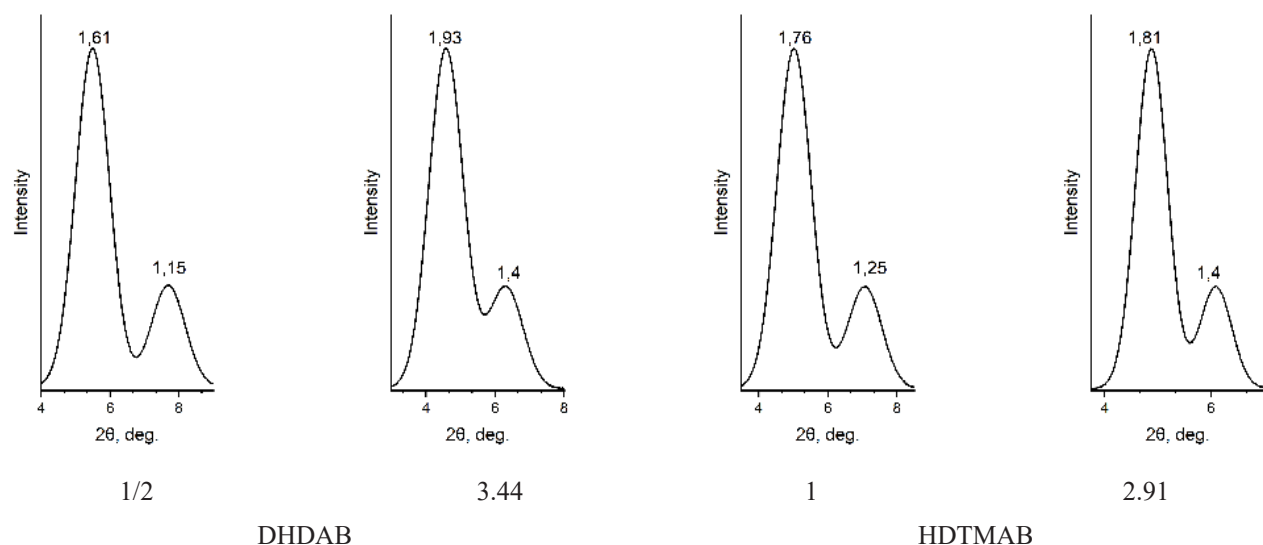


Fig. 9. X-ray diffraction patterns of organomodified sample MM70.

recorded interplanar distance does not exceed 2.35 nm.

Based on studies, it was established that the HDTMAB-B cation has a length of 2.53 nm, including a “nail head” with a length of 0.43 nm and a “nail body” with a length of 2.1 nm [30]. The “nail body” size varies between 0.41 and 0.46 nm, while the “nail head” has a size ranging from 0.51 to 0.67 nm, depending on the orientation of the carbon atoms of HDTMAB relative to the plane of montmorillonite - either along or across. Considering that the thickness of the montmorillonite (MM) layer is approximately 0.96 nm, the basal space of 1.85 nm in the analysed sample ( $n = 0.5 - 0.6$ ) corresponds to a lateral double arrangement of HDTMAB chains in the interlayer zone [31]. With further increase in basal space to 2.31 nm and above with  $n$  values up to 3.27, the possibility of a pseudo-trilayer arrangement of HDTMAB cations in the interlayer region is suggested.

Peaks in the X-ray diffraction patterns of MM86 and MM70 samples at all  $n$  values are characterized by a larger  $2\theta$  angle compared to MM. If the maximum  $d_{001}$  reflex values for MM86 and MM70 at  $n = 0.5$  are approximately 1.79 and 1.61 nm, respectively, for DHDAB, then upon saturation ( $n = 3.44$  and 3.2), they increase to 2.22 and 1.93 nm. While for MM86, the change in interlayer distance is around  $\sim 0.4$  nm, for MM70, these changes do not exceed 0.27 nm. In the former case, the assumption can be made about obtaining a complex structure from a double layer of DHDAB,

while in the latter case, the likely outcome is a single layer, but less ordered, with a reduced packing of their molecules.

At  $n = 1$ ,  $d_{001}$  is 1.83 nm for the MM86 sample and 1.76 nm for MM70, indicating an increase in the interpacket space of clay by an amount equivalent to two aliphatic chains. At the maximum filling level, approximately  $n = 2.91$  for HDTMAB -B in the MM86 sample and  $n = 3.00$  for MM70,  $d_{001}$  is 2.12 nm and 1.81 nm, respectively. At this stage, in both MM samples, the formation of a complex structure of HDTMAB -B molecules occur, where aliphatic chains are arranged in three layers parallel to the clay plates. At the same time, the polar parts of HDTMAB-B molecules occupy positions on the clay surface. In the context of HDTMAB-B adsorption, although MM70 shows a higher adsorption level compared to MM86, it is assumed that the volume of HDTMAB -B intercalated into the interlayer space of MM70 represents a smaller percentage of the total adsorbed surfactant. This assumption correlates with the observed lower values of interplanar distance for MM70.

#### Textural characteristics of modified montmorillonites

Organobentonites, representing bentonites modified with organic cations, play a crucial role in contemporary scientific and industrial activities due to their unique properties, such as increased hydrophobicity, improved rheological, and adsorption properties. However, for a

profound understanding of the potential applications of organobentonites and the optimization of their functionality, a detailed knowledge of their structure and texture is essential.

Low-temperature nitrogen adsorption is a key tool for assessing the porosity of materials, allowing the determination of the size, shape, and distribution of pores at the micro and meso levels. A thorough examination of textural characteristics will provide a better understanding of the mechanisms through which organic cations interact and modify the interlayer space of bentonite.

Nitrogen adsorption isotherms for the studied samples are presented in Fig. 10, and the parameters of the porous structure based on the obtained isotherms are listed in Table 1. Curves depicting the changes in the specific surface area of montmorillonite samples with respect to the  $n$  value are shown in Fig. 11.

In the MM-DHDAB system, as the value of  $n$

increases up to 0.25, the specific surface area increases from 53 to 68  $\text{m}^2 \text{g}^{-1}$ , but then starts decreasing to 24  $\text{m}^2 \text{g}^{-1}$  at  $n = 3.85$ . Similar changes are observed in the MM-HDTMAB systems.

For MM86 systems, the specific surface area increases to 65  $\text{m}^2 \text{g}^{-1}$  with the introduction of DHDAB at  $n = 0.25$  compared to the original MM86 (57  $\text{m}^2 \text{g}^{-1}$ ). At  $n = 3.44$ , it decreases to 20  $\text{m}^2 \text{g}^{-1}$ , and with HDTMAB saturation, the value is 26  $\text{m}^2 \text{g}^{-1}$  ( $n = 2.91$ ).

In the MM70 - DHDAB system, the increase in specific surface area is marginal, going from 48 to 49  $\text{m}^2 \text{g}^{-1}$  at  $n = 0.25$ , followed by a decrease to 19  $\text{m}^2 \text{g}^{-1}$  at  $n = 3.21$ . In the case of HDTMAB, the specific surface area increases from 48 to 53  $\text{m}^2 \text{g}^{-1}$  at  $n = 0.25$  and then decreases to 21  $\text{m}^2 \text{g}^{-1}$  at maximum saturation ( $n = 3$ ).

Therefore, the analysis of the obtained data indicates that the increase in the content of adsorbed surfactants (fraction of clay CEC  $n$ ) usually leads to an increase in the specific surface area at the initial stages (at small  $n$ ),

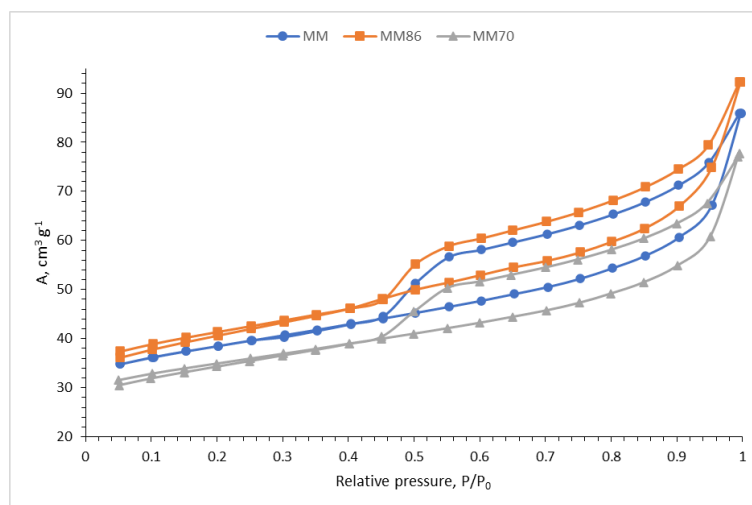
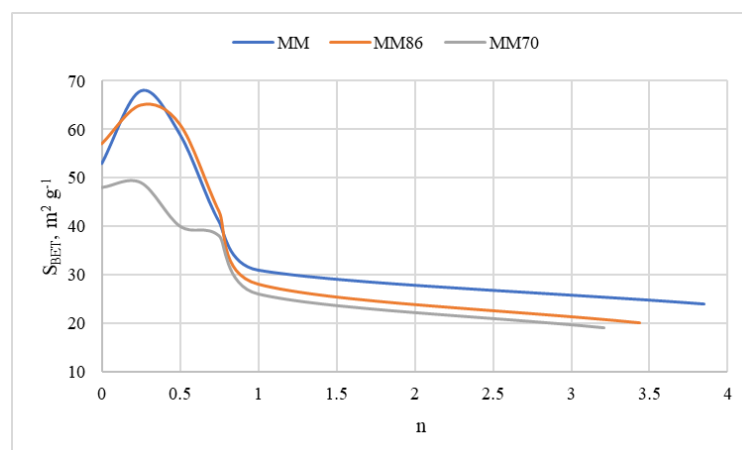


Fig. 10. Nitrogen adsorption isotherms on the samples.

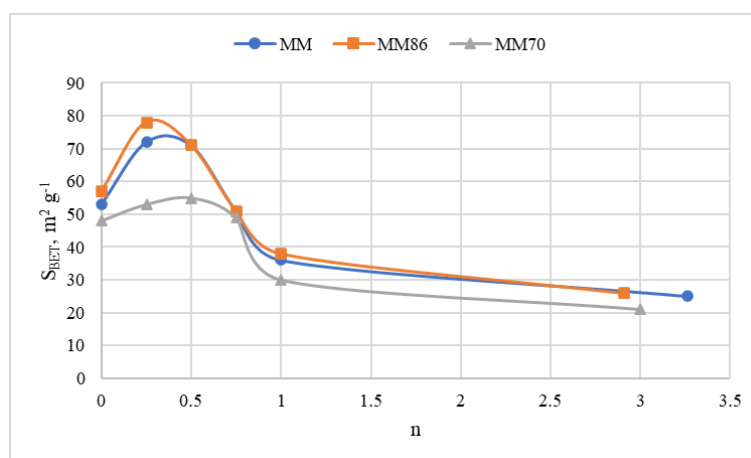
Table 1. Textural characteristics of the samples.

Sample	$S^1$ , $\text{m}^2 \text{g}^{-1}$	$S^2$ , $\text{m}^2 \text{g}^{-1}$	t-Plot*, $\text{m}^2 \text{g}^{-1}$	$V_{a^2}$ , $\text{cm}^3 \text{g}^{-1}$	$V_{b^2}$ , $\text{cm}^3 \text{g}^{-1}$	$R$ , Å	$D^{**}$ , Å	$D^{***}$ , Å
MM	53.13	52.19	0.941	52.19	0.087	44.6	14.23	4.39
MM86	57.07	56.03	1.031	0.040	0.093	44.1	14.33	4.40
MM70	48.01	47.17	0.894	0.033	0.079	44.7	14.37	4.41

<sup>1</sup> - specific surface area by BET; <sup>2</sup> - specific mesopore surface area,  $\text{m}^2 \text{g}^{-1}$ ; \* - external surface; \*\* - width of the average pore; \*\*\* - average micropore size;  $R$  - average pore size.



a)



b)

Fig. 11. Dependence of specific surface area on the value of n: (a) DHDAB; (b) HDTMAB.

which may suggest successful surfactant intercalation into the interlayer space of MM.

After a certain saturation threshold, further increase in the amount of surfactants leads to a reduction in specific surface area. This may be associated with the blocking of micropores or the formation of surfactant aggregates, reducing the available surface [32]. On average, HDTMAB demonstrates a higher specific surface area at similar n values compared to DHDAB, which may indicate a more efficient distribution or less aggregation of HDTMAB in the interlayer space.

Different MM samples (MM, MM86, MM70) exhibit distinct trends depending on the surfactant and their internal structure or chemical composition. Thus,

the choice of surfactant and its concentration influence the textural characteristics of organobentonites, which, in turn, can affect their functional properties and adsorption activity towards various adsorbates.

### Studying the adsorption activity of organobentonites towards methylene blue

Investigating the adsorption of MB is a pertinent focus in scientific research, driven by several key factors associated with determining the nature of the adsorbent material. The adsorption of methylene blue serves as a widely employed method for assessing the quality of organobentonites. The ability of bentonites to adsorb methylene blue can act as an indicator of their interlayer

charge and the presence of available active sites on the surface. The examination of methylene blue adsorption on organobentonites can enhance our understanding of the interaction between organic molecules and modified clay minerals.

Methylene blue is an organic dye that may enter water resources from various sources, such as the textile industry. Its removal from water is crucial from an environmental standpoint and for safeguarding public health.

The kinetics of the adsorption process were studied for a single concentration ( $50 \text{ mg L}^{-1}$ ), as depicted in Fig. 12.

For all montmorillonites (MM, MM86, and MM70), the initial concentration of MB was set at  $50 \text{ mg L}^{-1}$ . The MM sample, having the highest cation exchange capacity, also exhibits the greatest activity in the adsorption of methylene blue, especially in the early stages of the experiment. For MM, a comparatively faster adsorption is observed, with an adsorption rate of  $0.4 \text{ mg L}^{-1} \text{ min}^{-1}$  within the first 10 min, whereas for MM86 and MM70, it is  $0.15$  and  $0.1 \text{ mg L}^{-1} \text{ min}^{-1}$ , respectively. Thus, at the initial stages, the MM sample demonstrates the highest activity in methylene blue adsorption, while MM70 and MM86 show lower adsorption rates.

Over time, the adsorption rate decreases for all samples, likely associated with a reduction in the number of available adsorption sites on the montmorillonite surface. MM70, with the lowest cation exchange

capacity, exhibits the least activity in adsorption at all stages of the experiment. The adsorption rates in the later stages (90 - 120 min) are  $0.016$ ,  $0.018$ , and  $0.0067 \text{ mg L}^{-1} \text{ min}^{-1}$  for MM, MM86, and MM70, respectively. In the later stages, the adsorption rate decreases for all samples, but MM remains the most active in adsorption, although the difference with MM86 diminishes.

Thus, the data indicate a direct correlation between the cation exchange capacity of montmorillonite and its ability to adsorb methylene blue. This can be explained by the presence of a greater number of exchange sites enhancing the adsorption properties of the mineral.

Differences in the Adsorption Properties of Montmorillonites may be related to their structural characteristics, particularly the quantity of exchangeable cations; the higher the CEC of montmorillonite, the greater the speed and amount of adsorbed dye, which is consistent with previously known data [33]. If adsorption occurs solely due to ion exchange, the calculated values of the degree of exchangeable cation substitution for MM, MM86, and MM70 are  $18.75 \%$ ,  $15.49 \%$ , and  $10.27 \%$ , respectively.

The modification of montmorillonites with both surfactants led to a change in affinity for MB (Fig. 13 and 14). It was observed that for all modified samples, the degree of MB removal from the solution was higher compared to the corresponding unmodified samples, indicating an increase in the organophilicity of the inorganic matrix. In this case, the adsorption of the

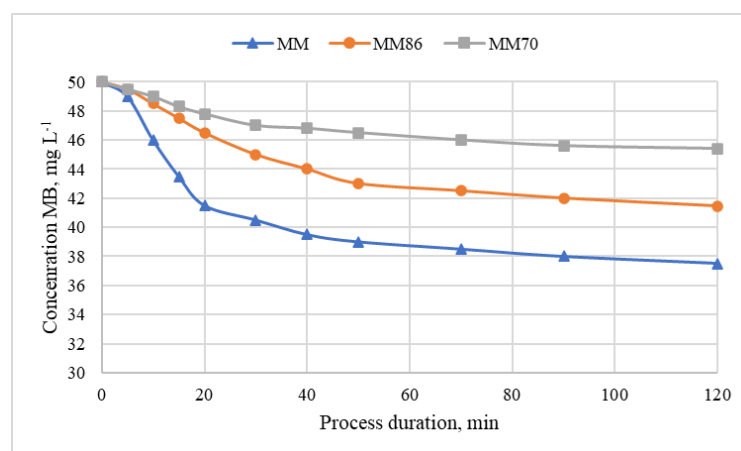


Fig. 12. Kinetics of methylene blue concentration reduction in the solution during the interaction of the studied samples.

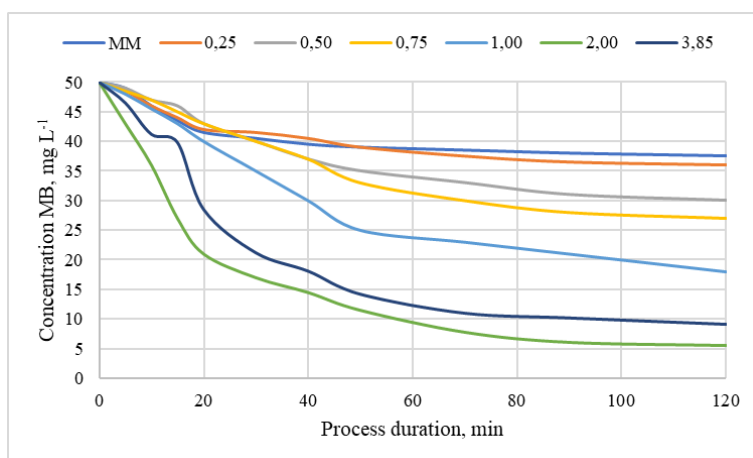


Fig. 13. Kinetics of methylene blue concentration reduction in the solution as a function of saturation degree ( $n$ ) with DHDAB.

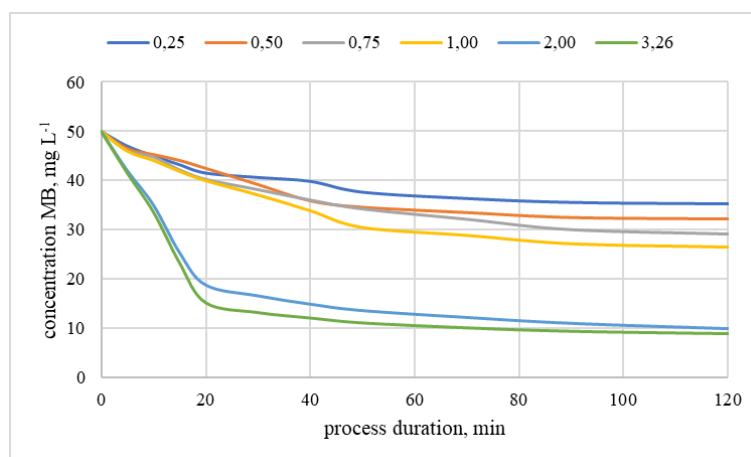


Fig. 14. Kinetics of methylene blue concentration reduction in the solution as a function of saturation degree ( $n$ ) with HDTMAB.

cationic dye may not solely occur through ion exchange but rather through the interaction of particles in the solution with the hydrophobic part of the surfactants introduced into the layers of montmorillonite [34].

Modification of montmorillonite with dihexadecyl-dimethylammonium bromide led to a noticeable change in the adsorption of methylene blue. In this case, MB adsorption likely occurs predominantly through ion exchange, aligning with traditional adsorption mechanisms on montmorillonites.

As seen in Fig. 13, for samples with  $n = 0.25 - 0.5$ , MB adsorption increases compared to the original

MM. This may be attributed not only to ion exchange but also to additional interactions between MB and the hydrophobic part of the surfactant. However, the effect of this interaction is not as pronounced as in subsequent samples.

At  $n = 0.75 \leq 2$ , a sharp increase in MB adsorption is observed, especially noticeable at  $n = 2$ . This indicates the predominance of adsorption mechanisms due to interactions with the hydrophobic part of the surfactant. Such an increase in adsorption could result from the formation of micellar structures or aggregates of surfactants in the interlayer space of MM, providing

additional sites for MB adsorption. However, despite further increases in saturation, the efficiency of MB adsorption decreases compared to  $n = 2$ . This could be linked to a denser packing of surfactant molecules in the interlayer space of MM, hindering access to adsorption sites for larger MB molecules. Additionally, excessive saturation may lead to the formation of micelles or surfactant aggregates that physically block access to interlayer spaces.

In the case of MM modification with hexadecyltrimethylammonium bromide at  $n = 0.25$ , a slight decrease in MB concentration in the solution is also observed over 120 min. This indicates moderate MB adsorption. Like the previous case, the highest efficiency in MB adsorption is observed at  $n \geq 1$ . This may be associated with an increased packing density of surfactant molecules in the interlayer space, creating optimal conditions for the adsorption of methylene blue cations. However, it is worth noting that despite the increase in saturation from 2 to 3.26, the difference in adsorption is not as significant, indicating potential saturation of adsorption sites or a reduction in the availability of adsorption sites due to a denser packing of surfactant molecules.

Studies conducted on samples MM86 and MM70 yielded results like MM. However, noteworthy is the reduction in the degree of methylene blue (MB) removal compared to the corresponding saturation degrees ( $n$ ) for MM. For instance, at the maximum saturation degree with dihexadecyldimethylammonium bromide for MM, a decrease in MB concentration is observed,

dropping to 18.24 % compared to 11.12 % for the MM sample with  $n = 2$ . For samples with lower CEC (Cation Exchange Capacity), the degree of MB removal increases with an increase in the saturation degree ( $n$ ). Thus, the MB concentration decreases from 21.2 % to 14.5 % for MM86 with  $n$  ranging from 2 to 3.44, and from 28.6 % to 21.8 % for MM70 with  $n$  changing from 2 to 3.21. In the context of modification with hexadecyltrimethylammonium bromide and saturation of these samples, the degree of MB removal reaches 82.1 % and 79.9 % for MM86 and MM70, respectively. It is essential to note that these values were achieved within a 120-minute interaction with the dye. Further extension of the adsorption time to 5 - 7 hours allows for up to 99 % removal of the dye from the solution.

Methylene blue adsorption isotherms for the studied samples are presented in Fig. 15 and 16.

The maximum adsorption of MB is  $16.5 \text{ mg g}^{-1}$  at a residual concentration of  $50 \text{ mg L}^{-1}$ . The efficiency of adsorption increases with an increase in the initial concentration of MB. Adsorption efficiency decreases with a reduction in the clay's Cation Exchange Capacity, i.e., in the order  $\text{MM} < \text{MM86} < \text{MM70}$ . MM86 reaches a maximum of  $14.5 \text{ mg g}^{-1}$  at an equilibrium concentration ( $C_1$ ) of  $40 - 42 \text{ mg L}^{-1}$ . At these equilibrium concentration values, the adsorption amount on MM70 reaches  $13.2 \text{ mg g}^{-1}$ . For their modified forms with  $n = 1$ , the adsorption amount reaches  $56.5$ ,  $50.2$ , and  $47.0 \text{ mg L}^{-1}$ . Further increasing  $n$  from 1 to saturation of the original montmorillonites does not alter the shape of the isotherm, only leading to

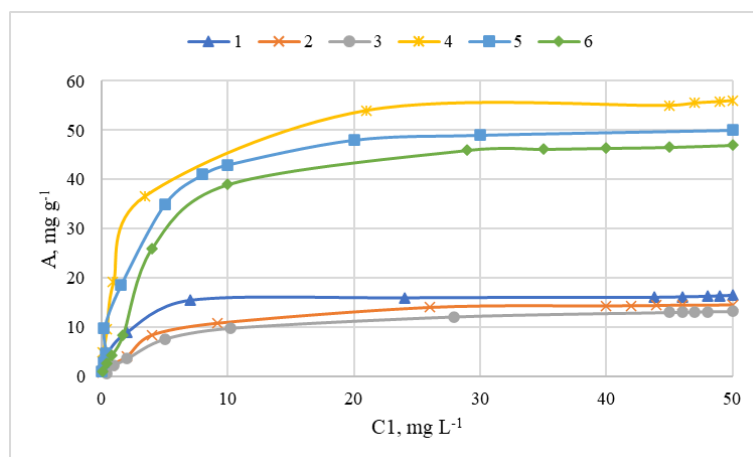


Fig. 15. Adsorption isotherms of methylene blue on: 1) MM; 2) MM86; 3) MM70, and on samples modified with DHDAB at saturation degree  $n = 1$ : 4) MM; 5) MM86; 6) MM70.

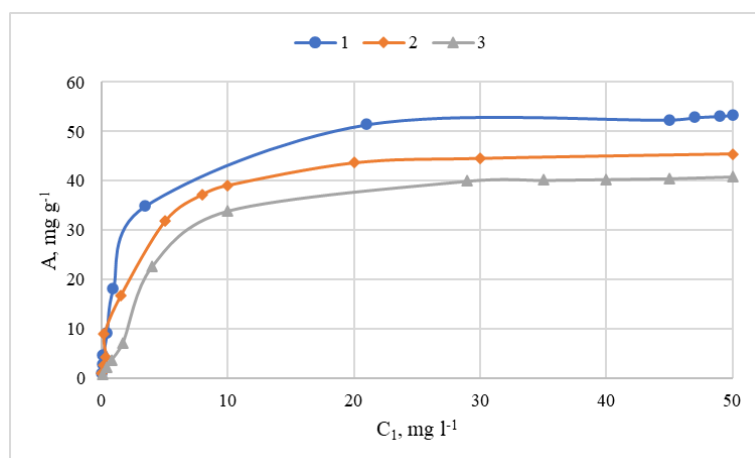


Fig. 16. Adsorption isotherms of methylene blue on samples modified with DHDAB at  $n = 1$ : 1) MM; 2) MM86; 3) MM70.

Table 2. Adsorption data of samples on methylene blue based on the Langmuir equation.

Sample	$A_0$ , mmol g <sup>-1</sup>	$K_L$	Surface Area, m <sup>2</sup> g <sup>-1</sup>	$\Sigma V$ , cm <sup>3</sup> g <sup>-1</sup>	R, nm
MM	0.052	57.854	33.082	0.0767	36.17
MM86	0.049	84.003	30.928	0.0744	38.69
MM70	0.047	46.736	29.697	0.0729	40.29
MM+ DHDAB	0.179	38.217	112.913	0.1223	10.59
MM86+ DHDAB	0.163	48.471	103.335	0.1153	11.58
MM70+ DHDAB	0.168	51.531	106.11	0.1119	11.27
MM+ HDTMAB	0.170	237.976	107.537	0.11187	20.806
MM86+ HDTMAB	0.157	45.228	99.331	0.11187	22.525
MM70+ HDTMAB	0.146	51.546	92.271	0.11187	24.248

changes in adsorption values. In this case, the obtained data replicate earlier findings when studying the kinetics of MB concentration changes (Fig. 11).

Based on these data, it can be inferred that the presence of dihexadecyldimethylammonium bromide (DHDAB) enhances the interaction between the montmorillonite surface and MB molecules, leading to increased adsorption efficiency. This may be associated with a change in the surface character of montmorillonite after modification. The introduction of hexadecyltrimethylammonium bromide also results in an increase in MB adsorption amounts compared to the original data, especially noticeable at low equilibrium concentration values.

The presented isotherms were characterized using

the Langmuir and BET equations, which are provided in Table 2.

Modification of montmorillonites with dihexadecyldimethylammonium bromide (DHDAB) increases the monolayer capacity ( $A_0$ ) by 3 - 4 times compared to the original samples. Among the original samples, MM exhibits the highest  $A_0$  value, while MM70 has the lowest. Modification also leads to an increase in the total pore volume, although not as radically as the specific surface area, and a decrease in the average pore size.

The modification of montmorillonites with DHDAB significantly enhances their adsorption capacity, as reflected in the increased specific surface area, total pore volume, and maximum adsorption amount. This can be explained by changes in the surface structure

and increased accessibility of adsorption sites due to the introduction of DHDAB.

Modification of montmorillonites with both agents enhances their adsorption properties. However, the choice of the agent and its interaction with a montmorillonite sample may vary, leading to differences in adsorption characteristics. Overall, modification using dihexadecyldimethylammonium bromide results in a higher value of  $A_0$  and a smaller pore radius.

## CONCLUSIONS

Sorption studies of DHDAB and HDTMAB complexes with montmorillonite have shown their high affinity to the interlayer space of clay. This process occurs in several stages: initial rapid saturation, saturation plateau, and subsequent super-equivalent sorption, which is likely associated with the formation of multilayer structures or micelle-like formations on the surface of clay plates. This sorption mechanism is characteristic for various cationic surfactants.

DHDAB with two alkyl chains demonstrates a more complex intercalation dynamic compared to HDTMAB, which, having only one chain, exhibits higher saturation efficiency at early stages.

Montmorillonite with lower CEC (cation exchange capacity) has fewer available sites for DHDAB intercalation, which is reflected in higher concentration values to achieve saturation plateau. However, HDTMAB shows less dependence on montmorillonite CEC in terms of sorption mechanism.

For DHDAB and HDTMAB, adsorption exceeds the CEC of montmorillonite by 3.16 and 2.87 times, respectively. With an increase in surfactant concentration in the solution up to 3 mmol/L, the adsorption of DHDAB and HDTMAB weakly changes, exceeding the CEC by 3.21 and 3.00 times, respectively.

For MM86 during saturation, the formation of a double layer of DHDAB is possible, while for MM70, it is more likely that a single layer of DHDAB is formed, but with less ordering and less dense molecular packing.

The efficiency of methylene blue adsorption on montmorillonites depends on their exchange capacity, structural characteristics, and degree of surfactant saturation. Interaction of methylene blue with the hydrophobic parts of surfactants plays an important role in adsorption, especially at certain degrees of

saturation. However, excessive saturation of surfactants can decrease the efficiency of adsorption due to blockage of the interlayer space.

*Authors' contributions: A.K. wrote the manuscript with support from A.A. and N.M.; O.M. and N.N. carried out the experiment.*

## REFERENCES

1. N. Vidal, C. Volzone, Influence of Organobentonite Structure on Toluene Adsorption from Water Solution, *Mater. Res.*, 15, 6, 2012, 944-953.
2. O. Carmody, R. Frost, Y. Xi and S. Kokot, Adsorption of hydrocarbons on organo-clays - Implications for oilspill remediation, *J. Colloid Interface Sci*, 305, 1, 2007, 17-24.
3. V.A. Gerasin, F.N. Bakhov, N.D. Merekalova, Y.M. Korolev, H.R. Fischer, E.M. Antipov, Structure of surfactant layers formed on  $\text{Na}^+$  montmorillonite and compatibility of the modified clay with polyolefins, *Polym. Sci. - Series A*, 47, 9, 2005, 954-967.
4. I. Fatimah, T. Huda, Preparation of cetyltrimethylammonium intercalated Indonesian montmorillonite for adsorption of toluene, *Appl. Clay Sci.*, 74, 2013, 115-120.
5. L. Paiva, A. Morales, R. Díaz, Organo-clays: properties, preparation, and applications, *Appl. Clay Sci.*, 42, 1, 2008, 8-24.
6. H. He, Y. Ma, J. Zhu, P. Yuan, P. Qing, Organo-clays prepared from montmorillonites with different cation exchange capacity and surfactant configuration, *Appl. Clay Sci.*, 48, 2010, 67-72.
7. Zh. Li, W. Jiang, H. Hong, An FTIR investigation of hexadecyltrimethylammonium intercalation into rectorite, *Spectrochimica Acta Part A*, 71, 4, 2008, 1525-1534.
8. C. Wu, X. Lou, X. Xu, A. Huang, M. Zhang, L. Ma, Thermodynamics and Kinetics of Pretilachlor Adsorption on Organobentonites for Controlled Release, *ACS Omega*, 5, 8, 2020, 4191-4199.
9. P. Palma, M. Köck-Schulmeyer, P. Alvarenga, L. Ledo, I.R. Barbosa, M.L. de Alda, D. Barceló, Risk assessment of pesticides detected in surface water of the Alqueva reservoir (Guadiana basin, southern of Portugal), *Sci. Total Environ.*, 488-489, 2014, 208-219.
10. J.H. Kim, W.S. Shin, Y.H. Kim, S.J. Choi, W.K.

- Jo, D.I. Song, Sorption and desorption kinetics of chlorophenols in hexadecyltrimethyl ammonium-montmorillonites and their model analysis, *Korean J. Chem. Eng.*, 22, 6, 2005, 857-864.
11. T. Bajda, Z. Klapysa, Adsorption of chromate from aqueous solutions by HDTMA-modified clinoptilolite, glauconite and montmorillonite, *Appl. Clay Sci.*, 86, 2013, 169-173.
12. H.B. Senturk, D. Ozdes, A. Gundogdu, C. Duran, M. Soylak, Removal of phenol from aqueous solutions by adsorption onto organomodified Tirebolu bentonite: Equilibrium, kinetic and thermodynamic study, *J. Hazard. Mater.*, 172, 1, 2009, 353-362.
13. T. Wang, J. Zhu, R. Zhu, F. Ge, P. Yuan, H. He, Enhancing the sorption capacity of CTMA-bentonite by simultaneous intercalation of cationic polyacrylamide, *J. Hazard. Mater.*, 178, 1-3, 2010, 1078-1084.
14. S.M. Lee, D. Tiwari, Organo and inorgano-organo-modified clays in the remediation of aqueous solutions: An overview, *Appl. Clay Sci.*, 59-60, 2012, 84-102.
15. P.J. Reeve, H.J. Fallowfield, The toxicity of cationic surfactant HDTMA-Br, desorbed from surfactant modified zeolite, towards faecal indicator and environmental microorganisms, *J. Hazard. Mater.*, 339, 2017, 208-215.
16. A.G. Thanos, A. Sotiropoulos, S. Malamis, E. Katsou, E.A. Pavlatou, Haralambous K.J. Regeneration of HDTMA-modified minerals after sorption with chromate anions, *Desalination Water Treat.*, 57, 57, 2016, 27869-27878.
17. A. Krajnak, E. Viglasova, M. Galambos, L. Krivosudsky, Kinetics, thermodynamics and isotherm parameters of uranium (VI) adsorption on natural and HDTMA-intercalated bentonite and zeolite, *Desalination Water Treat.*, 127, 2018, 272-281.
18. M. Andrunik, T. Bajda, Modification of Bentonite with Cationic and Nonionic Surfactants: Structural and Textural Features *Materials (Basel)*, 12, 22, 2019, 3772.
19. N. Nazhimova, O. Seitnazarova, A. Abdikamalova, Surfactant for Modification of Mineral Porous Materials and Their Porous Structure, *International Journal of Advanced Research in Science, Engineering and Technology*, 10, 7, 2023, 20894-20899.
20. J.A. Smith, P.R. Jaffe, C.T. Chiou, Effect of Ten Quaternary Ammonium Cations on Tetrachloromethane Sorption to Clay from Water, *Environ. Sci. Technol.*, 24, 8, 1990, 1167-1172.
21. L. Zhu, B. Chen, S. Tao, C.T. Chiou, Interactions of organic contaminants with mineral-adsorbed surfactants, *Environ. Sci. Technol.*, 37, 17, 2003, 4001-4006.
22. M. Okamoto, Recent advances in polymer/layered silicate nanocomposites: an overview from science to technology, *Mater. Sci. Technol.*, 22, 7, 2006, 756-779.
23. N.M. Boeva, Y.I. Bocharnikova, P.E. Belousov, V.V. Zhigarev, Determining the cation exchange capacity of montmorillonite by simultaneous thermal analysis method, *Russ. J. Phys. Chem.*, 90, 2016, 1525-1529.
24. J. Hrobáriková, J. Madejová, P. Komadel, Effect of heating temperature on Li-fixation, layer charge and properties of fine fractions of bentonites, *J. Mater. Chem.*, 11, 5, 2001, 1452-1457.
25. S. Azizian, S. Eris, Adsorption isotherms and kinetics, *Interface Science and Technology*, 33, 2021, 445-509.
26. A. Safavi, H. Abdollahi, N. Maleki, S. Zeinali, Interaction of anionic dyes and cationic surfactants with ionic liquid character, *J. Colloid Interface Sci.*, 322, 1, 2008, 274-280.
27. M. Khamis, B. Bulos, F. Jumean, A. Manassra, M. Dakiky, Azo dyes interactions with surfactants, Determination of the critical micelle concentration from acid-base equilibrium, *Dyes and Pigments*, 66, 2005, 179-183.
28. L. Heller-Kallai, Chapter 7.2 Thermally Modified Clay Minerals, *Developments in Clay Science*, 1, 2005, 289-308.
29. H. He, R.L. Frost, T. Bostrom, P. Yuan, L. Duong, D. Yang, Y. Xi, T. Klopogge, Changes in the morphology of organoclays with HDTMAC surfactant loading, *Appl. Clay Sci.*, 31, 3-4, 2006, 262-271.
30. L.M. Kaluderović, Z.P. Tomić, R.D. Đurović-Pejčev, P.J. Vulić, D.P. Ašanin, Influence of the organic complex concentration on adsorption of herbicide in organic modified montmorillonite, *Journal of Environmental Science and Health, Part B Pesticides Food Contaminants and Agricultural Wastes*, 52, 5, 2017, 291-297.

31. L. Zhu, X. Ruan, B. Chen, R. Zhu, Efficient removal and mechanisms of water-soluble aromatic contaminants by a reduced-charge bentonite modified with benzyltrimethylammonium cation, *Chemosphere*, 70, 11, 2008, 1987-1994.
32. K.J. Shah, M.K. Mishra, A.D. Shukla, T. Imae, D. Shah, Controlling wettability and hydrophobicity of organoclays modified with quaternary ammonium surfactants, *J. Colloid Interface Sci*, 407, 2013, 493-499.
33. H.B. Liu, H.N. Xiao, Investigation on intercalation modification of sodium-montmorillonite by cationic surfactant, *Int. J. Inorg. Mater.*, 27, 7, 2007, 780-784.
34. N. Mamataliev, A. Abdikamalova, I. Eshmetov, A. Kalbaev, Adsorption activity of pillared clays with respect to vapors of organic adsorbates, *J. Chem. Technol. Metall.*, 58, 6, 2023, 1028-1036.